Dalton Transactions

PAPER

View Article Online
View Journal | View Issue

Cite this: *Dalton Trans.*, 2018, **47**, 5055

Anti-tumour active gold(I), palladium(II) and ruthenium(II) complexes with thio- and selenoureato ligands: a comparative study†

Anja Molter,[a] Stefanie Kathrein,[b] Brigitte Kircher‡[b,c] and Fabian Mohr *‡[a]

Received 6th November 2017,
Accepted 10th March 2018

DOI: 10.1039/c7dt04180b

rsc.li/dalton

We report the results of a comparative study of the biological activity of a series of gold(I), palladium(II) and ruthenium(II) complexes containing deprotonated thio- and selenoureato ligands. A library of compounds was prepared and characterised by spectroscopic methods and the solid-state structures of several derivatives were determined by single crystal X-ray diffraction. The *in vitro* activity of these compounds was evaluated in mammary and ovarian carcinoma, acute lymphatic and acute and chronic myeloid leukemia cell lines. At lower concentrations Ru- and Pd-containing compounds displayed stronger anti-cancer effects than the gold compounds. In all cases, the selenium derivatives proved to be more active than the corresponding sulfur compounds.

Introduction

Acylselenoureas and acylthioureas of the type $ArC(O)NHC(E)NR_2$ (E = S, Se) have been known since the early 19th century[1,2] and their metal complexes, particularly those with acylthiourea ligands, have been thoroughly investigated for a number of applications.[3–6] For example, some acylthio- and acylselenoureas have been used for the extraction of gold from aqueous solutions.[7] Gold(I) complexes, especially those with phosphine ligands, are known to display biological activity.[8–14] A cytotoxicity study of a series of gold(I) triethylphosphine complexes $[Au(x)PEt_3]$ (X = Cl, Br, CN, SCN, or thiolato ligand) revealed that the sulfur containing complexes exhibited a higher activity compared to those containing halide ligands.[10] We have observed similar results in several gold(I) phosphine or N-heterocyclic carbene complexes containing heterocyclic sulfur ligands.[15,16] There are several reports describing studies of acylthiourea palladium complexes focusing on their anti-microbial,[17] fungicidal,[18] thermal[19] or mesomorphic[20] properties. Palladium(II) complexes with phenanthroline or its derivatives can intercalate with DNA thus exhibiting significant *in vitro* anti-tumour activity.[8,14,21–23] The anticancer activity of palladium complexes has recently been subject of a detailed review.[24] Apart from some homoleptic bis(selenoureato) palladium(II) complexes, there are only very few examples of heteroleptic Pd(II) derivatives containing monoanionic acylselenoureas.[6] Ruthenium compounds, in particular organometallic arene ruthenium(II) species, are emerging as a new class of promising anti-tumour active substances.[8,14,25–32] Ruthenium complexes with selenoureato ligands are unknown and only a few complexes with monoanionic thioureato ligands have been reported, although none have been examined for their biological properties.[33–38] Given our interest in the study of biologically active metal complexes with chalcogen ligands,[15,16,39–44] we wished to carry out a comparative study of a family of compounds containing metal centres with known anti-cancer activity [Au(PTA), Pd(1,10-Phen) and Ru(*p*-cymol)] in combination with both acylthio- and acylselenoureato ligands.

Results and discussion

Synthesis and crystal structures

The new selenourea *N*,*N*-diethyl-*N*′-4-nitrobenzoylselenourea (denoted hereafter as $\mathbf{HL^{Se}}$) was prepared from KSeCN, 4-nitrobenzoyl chloride and Et_2NH in CH_2Cl_2 in the presence of PEG-400 as phase-transfer catalyst following a literature procedure.[45] Orange crystals of the pure material were obtained in about 35% yield after recrystallisation from EtOH. Alternatively, the compound can also be obtained in similar yield using the original method of Douglass.[1] The known

[a]*Fakultät für Mathematik und Naturwissenschaften, Anorganische Chemie, Bergische Universität Wuppertal, 42119 Wuppertal, Germany. E-mail: fmohr@uni-wuppertal.de*
[b]*Innsbruck Medical University, Department of Internal Medicine V (Hematology & Oncology), Immunobiology and Stem Cell Laboratory, 6020 Innsbruck, Austria*
[c]*Tyrolean Cancer Research Institute, 6020 Innsbruck, Austria*

†Electronic supplementary information (ESI) available: Tables with crystallographic and refinement details, bond distances and angles as well as further information on the biological studies. CCDC 1584125–1584129. For ESI and crystallographic data in CIF or other electronic format see DOI: 10.1039/c7dt04180b

‡Both authors contributed equally to this work.

thiourea *N*,*N*-diethyl-*N*′-4-nitrobenzoylthiourea (denoted hereafter as $\mathbf{HL^S}$) was prepared analogously from KSCN, 4-nitrobenzoyl chloride and Et_2NH in acetone. The identity and purity of $\mathbf{HL^{Se}}$ was confirmed by ^1H, ^{13}C and ^{77}Se NMR spectroscopy as well as by single crystal X-ray diffraction. The molecular structure of the compound is shown in Fig. 1. Overall, the bond distances and angles of $\mathbf{HL^{Se}}$ (Table S1†) are similar to those reported for $PhC(O)NHC(Se)NEt_2$ [46] with some minor differences, which are detailed in the following section. The C=O and C=Se units in $\mathbf{HL^{Se}}$ lie almost perpendicular to each other (dihedral angle Se–C–N–C = 90.2°), whilst in the Ph-derivative this angle is approximately 108°.[46] Furthermore, the Ph-derivative forms dimers through intermolecular H-bonds between the NH group and the selenium atom in the solid-state, whereas $\mathbf{HL^{Se}}$ forms an infinite chain through N–H···O hydrogen bonds [N(H)···O = 2.905(3) Å]. In $\mathbf{HL^S}$ similar features can be observed: infinite chain formation through N–H···O hydrogen bonds [N(H)···O = 2.915(2) Å] and perpendicular C=O and C=S units (dihedral angle S–C–N–C = 91.1°).[47]

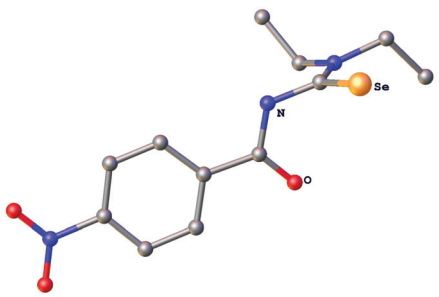

Fig. 1 Molecular structure of *N*,*N*-diethyl-*N*′-4-nitrobenzoylselenourea $\mathbf{HL^{Se}}$. Ellipsoids show 30% probability levels. Hydrogen atoms have been omitted for clarity.

The seleno- or thioureas $\mathbf{HL^{Se}}$ and $\mathbf{HL^S}$ react with [AuCl(PTA)] (PTA: 1,3,5-triaza-7-phosphaadamantane) in the presence of base to give neutral gold(I) PTA complexes containing the deprotonated seleno- or thioureato ligands (Scheme 1). Similarly, the reaction of $\mathbf{HL^{Se}}$ and $\mathbf{HL^S}$ with *cis*-[$PdCl_2$(1,10-Phen)] in the presence of base affords the cationic Pd(II) species *cis*-[Pd{4-$O_2NC_6H_4C(O)NC(E)NEt_2$}(1,10-Phen)]$^+$ (E = S, Se), which were isolated as their PF_6 salts as shown in Scheme 1. The organoruthenium(II) complexes [Ru{4-$O_2NC_6H_4C(O)NC(E)NEt_2$}(*p*-cymol)(PPh_3)]PF_6 (E = S, Se) were prepared from the reaction of [$RuCl_2$(*p*-cymol)]$_2$ with the corresponding ligand in the presence of Ph_3P, base and NH_4PF_6 (Scheme 1).

The compounds were characterised by ^1H, ^{13}C, ^{77}Se and ^{31}P NMR spectroscopy, electrospray mass spectrometry and several derivatives also by X-ray crystallography. In the gold(I) complexes the monoanionic thio- or selenoureato ligands coordinate only *via* the sulfur or selenium atom to the gold(I) centre. In case of the ruthenium and palladium species, bidentate coordination of both chalcogen atoms of the thio- and selenourea ligands is observed. In all the compounds reported here, the thio- or selenourea ligands are deprotonated, which is evident from the disappearance of the signal for the N–H proton in the ^1H NMR spectra of the compounds. For the gold derivatives, a shift of the position of the singlet due to the PTA ligand in the ^{31}P NMR spectra is observed upon coordination of the seleno- or thioureato ligands. This resonance is observed at −52.0 ppm in [AuCl(PTA)] and at −51.7 and −49.8 ppm in the thio- and selenoureato derivatives, respectively. In addition, the ^{13}C NMR signals of the quaternary carbon atom bound to the sulfur or selenium atom are shifted to 176.8 (S) or 167.1 (Se) ppm to higher field upon coordination. Whilst the ^{77}Se NMR signal for the unbound selenourea is found at 502 ppm, that of the gold selenoureato

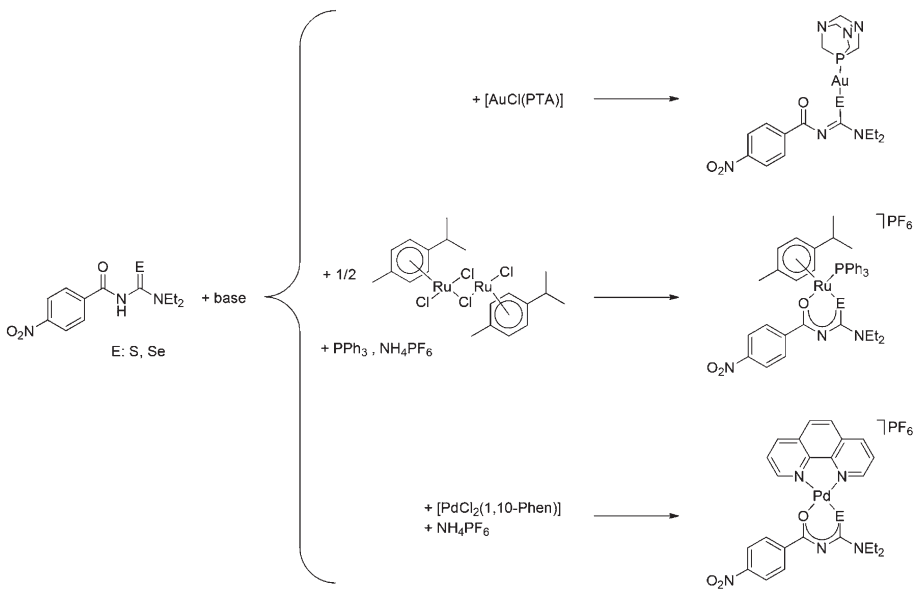

Scheme 1

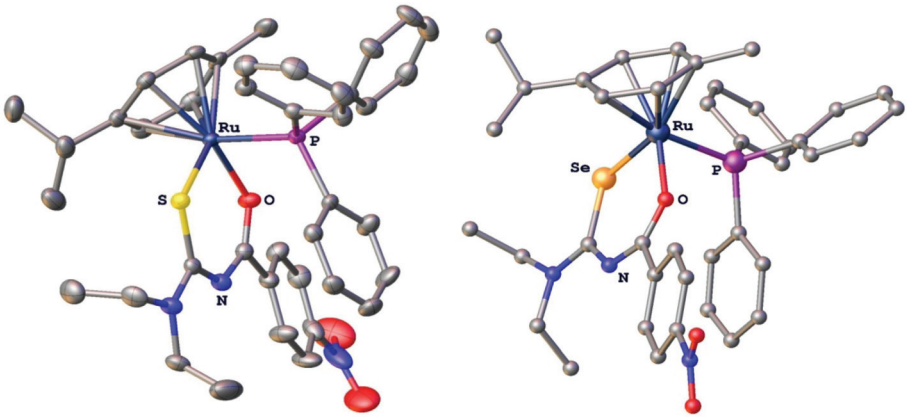

Fig. 2 Molecular structures of [Ru{4-$O_2NC_6H_4C(O)NC(S)NEt_2$}(*p*-cym)(PPh_3)]PF_6 and [Ru{4-$O_2NC_6H_4C(O)NC(Se)NEt_2$}(*p*-cym)($PPh_3$)]$PF_6$. Ellipsoids show 50% probability levels. Hydrogen atoms and the PF_6^- anions have been omitted for clarity.

species is observed at 244 ppm and that of the ruthenium derivative is shifted upfield to −26 ppm. Unfortunately, the palladium species were not soluble enough to obtain any ^{77}Se NMR spectra. The metal compounds were stable in solution for at least 48 h, as observed by NMR spectroscopy. Furthermore, we did not observe any ligand exchange reactions in dmso solutions. X-ray quality crystals of two ruthenium and palladium complexes were obtained and studied by X-ray diffraction. In the organoruthenium complexes (Fig. 2), the typical piano stool conformation about the metal centre is observed. The metal is thus bound to the arene ring (in η^6 fashion), the chelating thio- or selenoureato ligand as well as to the phosphorus atom of the PPh_3 ligand. The presence of four different atoms around the metal centre results in metal-centred chirality. The O–Ru–E angles (E = S, Se) are comparable to those reported for homoleptic, octahedral ruthenium(III) tris(chelate) complexes.[34] The distances between the ruthenium atom and the centre of the arene rings (S 1.745 Å, Se 1.746 Å) are typical for such η^6-arene ruthenium compounds.[48]

The palladium complexes (Fig. 3) show square-planar coordination with one bidentate chalcogenoureato and a 1,10-phenanthroline ligand bound to the metal. In both the ruthenium and the palladium compounds, the chalcogenoureato ligands are nearly planar due to electron delocalisation in the ligand backbone. A comparison of the two C–N distances as well as the C–O and C–Se bond lengths of the free and coordinated ligand, shows that upon coordination to the metal atom the NH–C═Se unit is transformed into an N═C–Se^- moiety (the selenolato tautomer). The C–Se bond distance increases from 1.82 Å to 1.88 Å (Pd) or 1.90 Å (Ru) which is in agreement with literature data for ruthenium-μ-phenylselenido compounds.[49] Due to the slightly smaller radius of the sulfur atom, the analogous bond distances in the sulfur complexes are correspondingly shorter. The C–S bond distance increases from 1.66 Å (**HL^S**) to 1.73 Å in the complex. In contrast, the C═O and C(O)N bond distances remain virtually unchanged upon coordination when compared with those of the free seleno- or thiourea, respectively. A table listing important

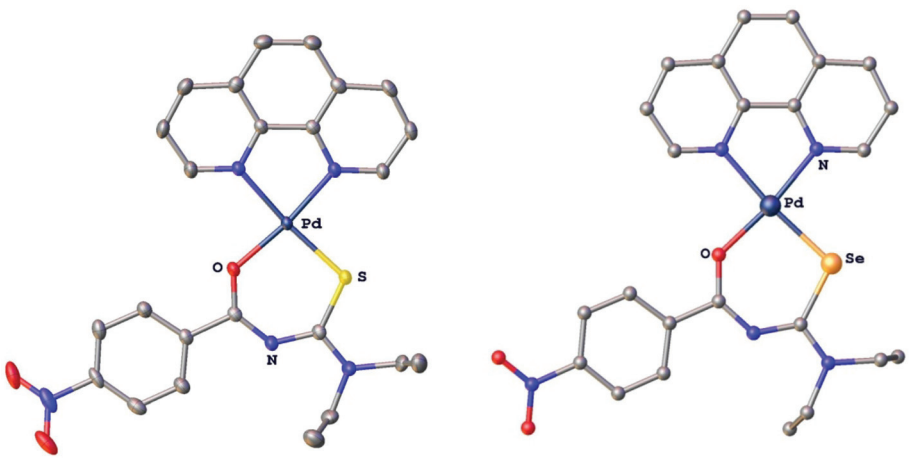

Fig. 3 Molecular structures of *cis*-[Pd{4-$O_2NC_6H_4C(O)NC(S)NEt_2$}(1,10-phen)]PF_6 and *cis*-[Pd{4-$O_2NC_6H_4C(O)NC(Se)NEt_2$}(1,10-phen)]$PF_6$. Ellipsoids show 50% probability levels. Hydrogen atoms, the PF_6^- anions as well as the dmso of solvation have been omitted for clarity.

bond distances and angles of the metal complexes and the thio- and selenourea ligands is included in the ESI.†

Biological studies

The biological activity of $\mathbf{HL^S}$, $\mathbf{HL^{Se}}$ as well as selected Au(I), Pd(II) and Ru(II) complexes including their chlorido-precursors (Chart 1) and cisplatin as further control was determined by their effect on proliferation, metabolic activity, programmed cell death and induction of oxidative stress of various tumor and leukemia cell lines.

All Au(I), Pd(II) and Ru(II) compounds dose-dependently reduced the proliferation of mammary and ovarian carcinoma, acute lymphatic as well as acute and chronic myeloid leukemia cell lines (ESI Fig. S1A–S1F†), whereby, in general, the selenium derivatives induced stronger effects than the sulfur compounds. For example, a concentration of 5 μM **Pd–S** significantly reduced the proliferation of SUP-B15 cells from 100% (without compound; data not shown) to 44.5 ± 8.4% and a concentration of 10 μM to 18.7 ± 3.1% (p < 0,05; Fig. 4) so that the IC50 was calculated as 4.9 ± 1.2 μM (Table 1). Interestingly, in the mammary carcinoma as well as the myeloid leukemia cell lines **Pd–S** was almost ineffective. In contrast, **Pd–Se** induced strong anti-proliferative effects and both Ru(II) compounds completely abolished the proliferation in all cell lines tested. Weaker anti-proliferative activity (again in all cell lines) was observed for the two Au(I) complexes. Cisplatin dose-dependently reduced the proliferation of the tumor cell lines, but did not show any activity on the leukemia cell lines. Whereas $[RuCl_2(p\text{-cymol})]_2$ was completely ineffective in all cell lines, [AuCl(PTA)] and the thio- and selenoureas $\mathbf{HL^{Se}}$ and $\mathbf{HL^S}$ induced anti-proliferative effects at higher concentrations (25 μM and 50 μM, ESI Fig. S1A–S1F†). *cis*-

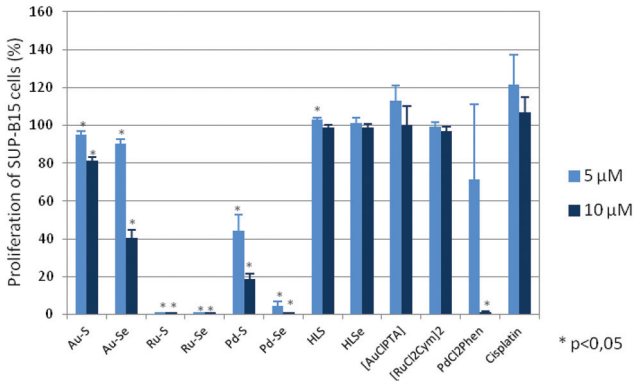

Fig. 4 Proliferation of SUP-B15 cells after a three-day incubation with the Au(I), Ru(II), Pd(II) complexes, $\mathbf{HL^S}$, $\mathbf{HL^{Se}}$, the chlorido complexes [AuCl(PTA)], $[RuCl_2(p\text{-cymol})]_2$, *cis*-$[PdCl_2(1,10\text{-Phen})]$ as well as cisplatin. Proliferation in the absence of the compounds was set to 100%. Mean proliferation and standard error of four experiments is shown. Statistical significance was determined with the Wilcoxon Rank Sum Test (*p < 0.05 against the untreated control).

Table 1 IC50 values of the metal complexes in SUP-B15 cells

	IC50 (μM)	
Compound	Proliferation	Metabolic activity
Au–S	17.9 ± 3.2	18.6 ± 3.2
Au–Se	9.1 ± 0.5	10.4 ± 1.0
Ru–S	3.5 ± 0.2	3.7 ± 0.7
Ru–Se	2.6 ± 0.5	4.1 ± 0.2
Pd–S	4.9 ± 1.2	13.9 ± 1.9
Pd–Se	3.7 ± 0.4	4.4 ± 0.0

IC50 values are calculated as the concentration at which the compounds induce 50% inhibition of proliferation or metabolic activity of SUP-B15 cells in comparison to untreated cells. The IC50 values are presented as means ± standard error of four experiments.

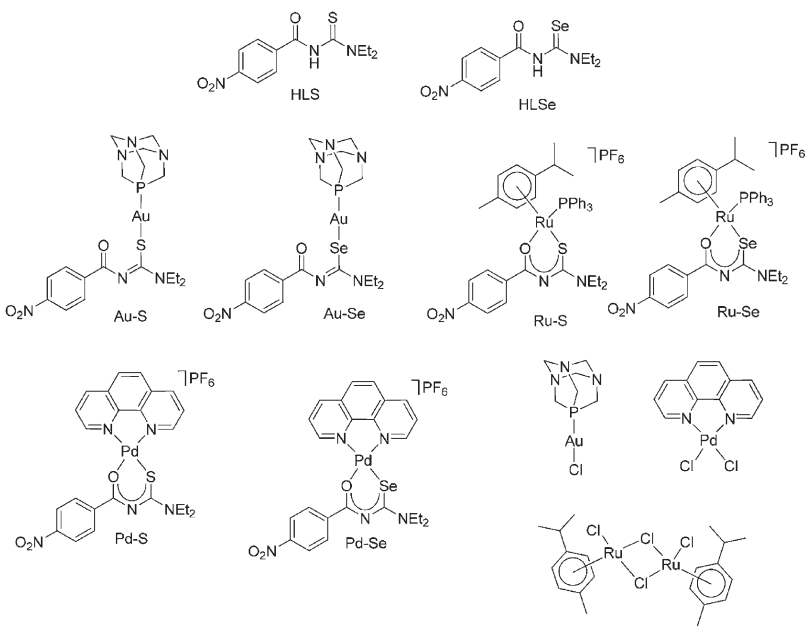

Chart 1 Compounds selected for biological studies.

[$PdCl_2$(1,10-Phen)] dose-dependently reduced the proliferation of all cell lines almost as effective as **Pd–Se** which may be explained by the ability of *cis*-[$PdCl_2$(1,10-Phen)] to intercalate with DNA.

The anti-proliferative activity of the substances was also examined on A-2780 cells resistant to cisplatin and revealed that the Au(I), Pd(II) and Ru(II) compounds have the potential to overcome cisplatin resistance (Table 2).

To evaluate if the reduced cell growth was also accompanied by cell death, the metabolic activity of the cell lines after compound incubation was analysed. Metabolic activity is determined by the reduction of tetrazolium salts into formazan derivatives. Since this process requires functional mitochondria, the assay discriminates living and dead cells whose mitochondria are deactivated within a few minutes after cell death. As shown in Fig. 5 and ESI Fig. S2A–S2F,† the metabolic activity of the cell lines was also dose-dependently diminished after 72 hours of incubation with the test compounds and *cis*-[$PdCl_2$(1,10-Phen)]. Again, the Ru(II) compounds and **Pd–Se** were the most active compounds with an IC50 of ~4 μM (Table 1), whereas the chlorido precursors [AuCl(PTA)] and [$RuCl_2$(*p*-cymol)]$_2$, HL^S, HL^{Se} as well as cisplatin were almost ineffective.

To confirm the cytotoxicity of the compounds, their capacity to induce programmed cell-death was determined by ssDNA apoptosis ELISA, which is based on the selective denaturation of DNA in apoptotic cells by formamide and further detection of denatured DNA with a monoclonal antibody to single-stranded DNA (ssDNA). Compounds which reduced proliferation and metabolic activity also induced apoptosis of the leukemia and tumor cells, whereby the sensitivity of the cell lines to programmed cell-death induction varied (ESI Fig. S3A–S3E†). For example, apoptosis of the cell line SUP-B15 was 3.7 ± 0.8 times higher after addition of 5 μM **Pd–Se** and 5.2 ± 0.6 times higher when 10 μM **Pd–Se** was added to the cultures in comparison to cells without compound incubation (Fig. 6).

A similar pro-apoptotic effect was observed for both Ru(II) compounds, whereas 10 μM **Au–Se** and 5 μM as well as 10 μM

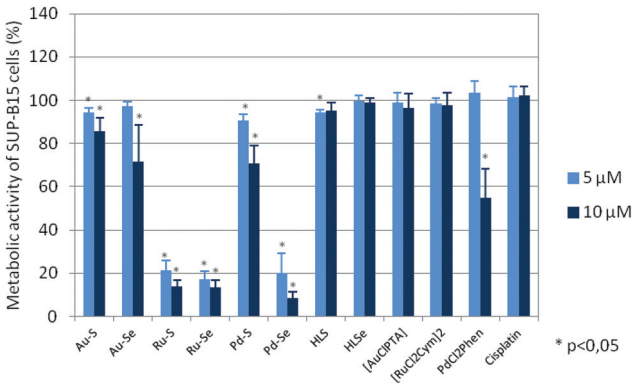

Fig. 5 Metabolic activity of SUP-B15 cells after a three-day incubation with the Au(I), Ru(II), Pd(II) complexes, HL^S, HL^{Se}, [AuCl(PTA)], [$RuCl_2$(*p*-cymol)]$_2$, *cis*-[$PdCl_2$(1,10-Phen)] as well as cisplatin. Metabolic activity in the absence of the compounds was set to 100%. Mean metabolic activity and standard error of four experiments is shown. Statistical significance was determined with the Wilcoxon Rank Sum Test (*$p < 0.05$ against the untreated control).

Pd–S caused a lower, but significant apoptosis rate. Consistent with the weak anti-proliferative and anti-metabolic activity, incubation with **Au–S** did not lead to programmed cell death in any of the cell lines. [AuCl(PTA)], [$RuCl_2$(*p*-cymol)]$_2$ and cisplatin were also ineffective in inducing apoptosis. Interestingly, despite no activity on proliferation and metabolism, HL^S and HL^{Se} significantly induced apoptosis in all leukemic cell lines, but not in the carcinoma cell lines (Fig. 6 and ESI Fig. S3A–S3E†). A similar effect was observed for *cis*-[$PdCl_2$(1,10-Phen)], which decreased proliferation and metabolic activity of the cell lines, however, without inducing their cell death. These rather contradictory results are currently under investigation.

The pro-apoptotic effect of **Ru–Se** (Fig. 7A) and the lacking effect of [$RuCl_2$(*p*-cymol)]$_2$ (Fig. 7B) can be readily detected by morphological changes of the cisplatin-resistant A-2780 cells.

One mechanism involved in the induction of apoptosis is oxidative stress triggered by the formation of reactive oxygen

Table 2 Proliferation of the cisplatin-sensitive and the cisplatin-resistant ovarian carcinoma cell line A-2780 after a three-day incubation with the Au(I), Ru(II), Pd(II) complexes, HL^S, HL^{Se}, the chlorido complexes [AuCl(PTA)], [$RuCl_2$(*p*-cymol)]$_2$, *cis*-[$PdCl_2$(1,10-Phen)] and cisplatin. Proliferation in the absence of the compounds was set to 100%. One representative experiment is shown

Compound 5 μM	A-2780		Compound 10 μM	A-2780	
	Cisplatin-sensitive	Cisplatin-resistant		Cisplatin-sensitive	Cisplatin-resistant
Au–S	46.8	79.8	**Au–S**	37.0	28.1
Au–Se	11.7	12.2	**Au–Se**	0.1	3.2
Ru–S	0.1	0.6	**Ru–S**	0.0	0.2
Ru–Se	0.1	0.2	**Ru–Se**	0.0	0.1
Pd–S	1.0	1.5	**Pd–S**	0.1	0.2
Pd–Se	0.2	0.3	**Pd–Se**	0.0	0.1
HL^S	80.2	92.4	HL^S	74.4	111.6
HL^{Se}	76.2	91.7	HL^{Se}	66.5	108.7
AuClPTA	107.2	76.8	AuClPTA	80.9	88.6
$[Cl_2Cym]_2$	84.7	97.1	$[Cl_2Cym]_2$	97.1	83.8
$PdCl_2$Phen	24.1	66.4	$PdCl_2$Phen	14.3	54.1
Cisplatin	15.0	67.2	Cisplatin	9.1	64.9

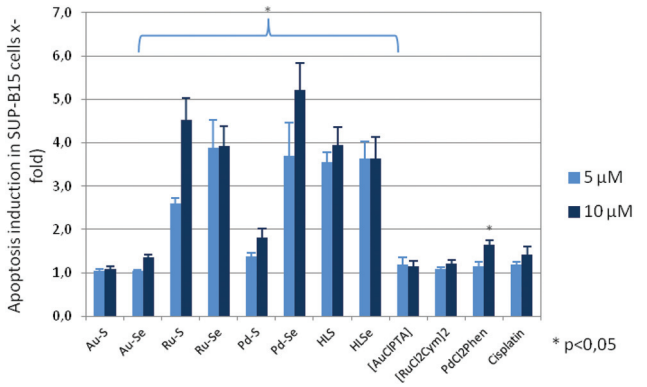

Fig. 6 Induction of apoptosis in SUP-B15 cells after a three-day incubation with the Au(I), Ru(II), Pd(II) complexes, $\mathbf{HL^S}$, $\mathbf{HL^{Se}}$, [AuCl(PTA)], $[RuCl_2(p\text{-cymol})]_2$, *cis*-$[PdCl_2(1,10\text{-Phen})]$ as well as cisplatin. Mean apoptosis induction (x-fold) and standard error of four experiments is shown. Apoptosis rate in the absence of the respective compound was set to 1. Statistical significance was determined with the Wilcoxon Rank Sum Test (*$p < 0.05$ against the untreated control).

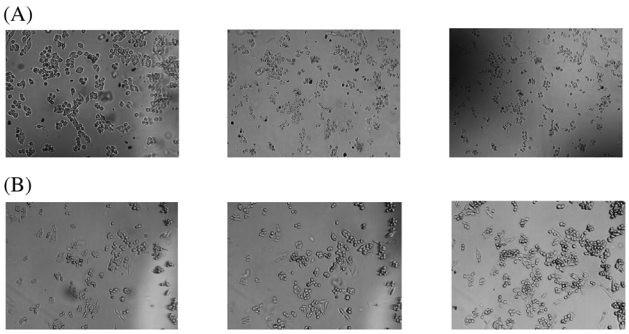

Fig. 7 Morphologic changes after a one-hour and 24-hours incubation, respectively, with 10 µM **Ru–Se** (A) and 10 µM $[RuCl_2(p\text{-cymol})]_2$ (B). One representative experiment is shown.

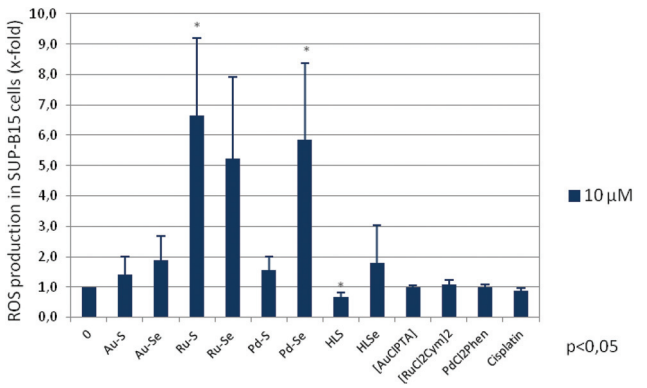

Fig. 8 Induction of oxidative stress in SUP-B15 cells after a two-hours incubation with the Au(I), Ru(II), Pd(II) complexes, $\mathbf{HL^S}$, $\mathbf{HL^{Se}}$, [AuCl(PTA)], $[RuCl_2(p\text{-cymol})]_2$, *cis*-$[PdCl_2(1,10\text{-Phen})]$ as well as cisplatin. Mean ROS production (x-fold) with standard error of six (for the chloro precursors and cisplatin four) experiments is shown. Statistical significance was determined with the Wilcoxon Rank Sum Test (*$p < 0.05$ against the untreated control).

species (ROS) due to deregulated mitochondrial activity. It has been shown for a variety of gold,[50–52] ruthenium[31,32,53–55] and palladium[56] complexes that their anti-tumour activity is mediated by an enhanced ROS production. Therefore, ROS levels were measured after a two-hour incubation of SUP-B15 cells with 10 µM of the respective compound. As shown in Fig. 8, both Ru(II) compounds and **Pd–Se** significantly induced oxidative stress in this cell line, in agreement with an increase of programmed cell death. Interestingly, the pro-apoptotic effect of $\mathbf{HL^S}$ and $\mathbf{HL^{Se}}$ cannot be explained by an increase in ROS formation. Neither the chlorido compounds nor cisplatin did induce oxidative stress of SUP-B15 cells.

Conclusions

In summary, gold(I), palladium(II) and ruthenium(II) compounds containing anionic nitro-substituted acylseleno- or acylthioureas display strong anti-tumor and anti-leukemia effects. The ligands $\mathbf{HL^S}$, $\mathbf{HL^{Se}}$ as well as the chlorido complexes [AuCl(PTA)] and $[RuCl_2(p\text{-cymol})]_2$ induced only weak effects or only at the highest concentrations tested, whereas *cis*-$[PdCl_2(1,10\text{-Phen})]$ reduced the proliferation and the metabolic activity almost as effective as the test compounds. The mechanisms of action include inhibition of proliferation and metabolic activity as well as induction of apoptosis and oxidative stress by ROS formation. The strongest effects were observed for the Ru(II) compounds followed by the Pd(II) complexes whereby the selenium-containing compounds displayed stronger biological activity than the sulfur derivatives. The Au(I) complexes were only effective at higher concentrations.

Materials and methods

Chemistry

Unless otherwise stated, all manipulations were carried out without taking precautions to exclude air and moisture. All chemicals and solvents (HPLC quality) were sourced commercially and used as received. [AuCl(PTA)] was prepared from the reaction of [AuCl(tht)][57] with the appropriate amount of the phosphine. The other metal precursors *cis*-$[PdCl_2(1,10\text{-phen})]$,[58] $[Ru(p\text{-cymol})Cl_2]_2$ [59] as well as *N*,*N*-diethyl-*N*′-4-nitrobenzoylthiourea ($\mathbf{HL^S}$)[60] were prepared by standard procedures described in the literature. The purity of all compounds was confirmed to be >95% by elemental analysis or high-resolution mass spectrometry.

Instrumentation

NMR spectroscopy. ^1H, ^{13}C, ^{77}Se and $^{31}P\{^1H\}$ NMR spectra were recorded on 400 Bruker Avance or 600 MHz Bruker Avance II spectrometers. Chemical shifts are quoted relative to external $SiMe_4$ (^1H, ^{13}C), Me_2Se or KSeCN (^{77}Se) and 85% H_3PO_4 (^{31}P).

IR spectroscopy. IR spectra were run as KBr pellets on a Bruker Tensor 27 instrument.

Elemental analyses. Elemental analyses were performed by staff of the in-house microanalytical laboratory using an Elementar Vario EL analyser.

Mass spectrometry. High-resolution electrospray mass spectra were recorded on Bruker MicroTOF spectrometer in positive ion mode using solutions of the samples in MeCN.

X-ray crystallography. Diffraction data were collected at 150 K using a Rigaku Oxford Diffraction Gemini E Ultra diffractometer, equipped with an EOS CCD area detector and a four-circle kappa goniometer. For the data collection the Mo source emitting graphite-monochromated Mo-Kα radiation (λ = 0.71073 Å) was used. Data integration, scaling and empirical absorption correction was carried out using the CrysAlis Pro program package.[61] The structures were solved using Direct Methods or Patterson Methods and refined by Full-Matrix-Least-Squares against F^2. The non-hydrogen atoms were refined anisotropically and hydrogen atoms were placed at idealized positions and refined using the riding model. All calculations were carried out using the program Olex2.[62] Full crystallographic and refinement details as well as tables with bond lengths and angles are included in the ESI.†

Syntheses

***N*,*N*-Diethyl-*N*′-4-nitrobenzoylselenourea (HL^{Se}).** To a suspension of KSeCN (2.88 g, 20 mmol) and PEG-400 (0.28 mL) in CH_2Cl_2 (10 mL) was added a solution of 4-nitrobenzoyl chloride (3.71 g, 20 mmol) in CH_2Cl_2 (20 mL). After *ca.* 15 min at room temperature Et_2NH (2.07 mL, 20 mmol) was added, and the resulting mixture was stirred for 1 h protected from light. The red-orange mixture was filtered and the filtrate subsequently evaporated to dryness. The resulting solid was recrystallised from EtOH to give 2.29 g (35%) orange crystals. X-ray quality crystals were selected from this bulk sample.

^{1}H NMR (400 MHz, $CDCl_3$): δ = 1.33 (t, J = 7.1 Hz, 3H, NCH_2CH_3), 1.41 (t, J = 6.3 Hz, 3H, NCH_2CH_3), 3.60 (br. s, 2H, NCH_2CH_3), 4.14 (br. s, 2H, NCH_2CH_3), 8.03 (d, J = 8.2 Hz, 2H, H-2), 8.32 (d, J = 8.2 Hz, 2H, H-3), 8.65 (br. s, 1H, NH) ppm. ^{13}C{^{1}H} NMR (101 MHz, $CDCl_3$): δ = 11.6 (NCH_2CH_3), 12.9 (NCH_2CH_3), 48.6 (NCH_2CH_3), 51.4 (NCH_2CH_3), 124.1 (C-3), 129.1 (C-2), 137.9 (C-1), 150.4 (C-4), 160.4 (C=O), 179.8 (C=Se) ppm. ^{77}Se NMR (76 MHz, $CDCl_3$): δ = 502 ppm. IR (KBr disk) ν: 1347 (s, NO_2), 1526 (s, NO_2), 1649 (s, C=O amido urea), 2933 (w, C_{sp^3}–H), 2975 (w, C_{sp^3}–H), 3055 (w, C_{sp^2}–H), 3289 (m, N–H) cm^{-1}. Elemental analysis calcd (%) for $C_{12}H_{15}N_3O_3Se$ (328.23 g mol^{-1}): C 43.91, H 4.61, N 12.80; found C 43.22, H 4.49, N 13.02.

Preparation of the gold(I) complexes

[Au{4-O$_2$NC$_6$H$_4$C(O)=NC(Se)NEt$_2$}(PTA)]. HL^{Se} (92.7 mg, 0.28 mmol) and NaOMe (16.8 mg, 0.31 mmol) were dissolved in methanol (10 mL) under dinitrogen. The clear orange solution was stirred for 20 min at room temperature, then [AuCl(PTA)] (100 mg, 0.26 mmol) was added to give a yellow suspension. After 18 h at room temperature, the yellow solution with little black precipitate was evaporated to dryness. The residue was taken up in dichloromethane, passed through Celite and concentrated in vacuum. Addition of diethyl ether afforded a yellow solid, which was isolated by filtration and dried in air. Yield: 0.150 g (86%). ^{1}H NMR (400 MHz, $CDCl_3$): δ = 1.28 (br. s, 6H, NCH_2CH_3), 3.66 (br. s, 2H, NCH_2CH_3), 3.81 (br. s, 2H, NCH_2CH_3), 4.02 (s, 6H, NCH_2N), 4.42 (q, $^2J_{H-H}$ = 13.2 Hz, 6H, PCH_2N), 8.21 (d, J = 8.9 Hz, 2H, H-3), 8.28 (d, J = 8.9 Hz, 2H, H-2) ppm. ^{31}P{H} NMR (162 MHz, $CDCl_3$): δ = −49.8 ppm. ^{13}C{H} NMR (101 MHz, $CDCl_3$): δ = 13.0 (NCH_2CH_3), 13.4 (NCH_2CH_3), 46.0 (NCH_2CH_3), 48.4 (NCH_2CH_3), 52.3 (d, $^1J_{P-C}$ = 18.7 Hz, PCH_2N), 72.9 (d, $^3J_{P-C}$ = 7.7 Hz, NCH_2N), 123.1 (C-2), 130.2 (C-3), 143.68 (C-4), 149.2 (C-1), 163.1 (C=O), 167.1 (C–Se) ppm. ^{77}Se NMR (76 MHz, $CDCl_3$, Me_2Se): 244 ppm. IR (KBr disk) ν: 1342 (s, NO_2), 1520 (s, NO_2), 2932 (m, C_{sp^3}–H), 2972 (m, C_{sp^3}–H), 3058 (w, C_{sp^2}–H) cm^{-1}. Elemental analysis calcd (%) for $C_{18}H_{26}AuN_6O_3PSe$ (681.34 g mol^{-1}): C 31.73, H 3.85, N 12.33; found: C 31.64, H 4.16, N 11.83.

[Au{4-O$_2$NC$_6$H$_4$C(O)=NC(S)NEt$_2$}(PTA)]. This was prepared as above using HL^{S} (79.4 mg, 0.28 mmol), NaOMe (16.8 mg, 0.31 mmol) and [AuCl(PTA)] (100 mg, 0.26 mmol). The product was obtained as yellow solid in 83% yield (0.135 g). ^{1}H NMR (400 MHz, $CDCl_3$): δ = 1.26 (br. s, 6H, NCH_2CH_3), 3.63 (br. s, 2H, NCH_2CH_3), 3.80 (br. s, 2H, NCH_2CH_3), 4.02 (s, 6H, NCH_2N), 4.40 (AB-q, $^2J_{H-H}$ = 13.2 Hz, 6H, PCH_2N), 8.24 (4H, H-2, H-3) ppm. ^{31}P{^{1}H} NMR (162 MHz, $CDCl_3$): δ = −51.7 ppm. ^{13}C{^{1}H} NMR (101 MHz, $CDCl_3$): δ = 12.9 (NCH_2CH_3), 46.1 (NCH_2CH_3), 46.5 (NCH_2CH_3), 51.9 (d, $^1J_{P-C}$ = 20.0 Hz, PCH_2N), 72.8 (d, $^3J_{P-C}$ = 7.9 Hz, NCH_2N), 123.0 (C-2), 129.9 (C-3), 143.8 (C-1), 149.0 (C-4), 166.0 (C=O), 176.8 (C–S) ppm. IR (KBr disk) ν: 1343 (s, NO_2), 1518 (s, NO_2), 1567 (s, C=O), 2933 (w, C_{sp^3}–H), 2970 (w, C_{sp^3}–H), 3067 (w, C_{sp^2}–H) cm^{-1}. Elemental analysis calcd (%) for $C_{18}H_{26}AuN_6O_3PS$ (634.44 g mol^{-1}): C 34.08, H 4.13, N 13.25, S 4.86; found: C 33.75, H 4.44, N 12.77, S 4.86.

Preparation of the palladium(II) complexes

***cis*-[Pd{4-NO$_2$C$_6$H$_4$C(O)NC(Se)NEt$_2$}(1,10-Phen)]PF$_6$.** A mixture containing [PdCl$_2$(1,10-Phen)] (50.0 mg, 0.14 mmol), HL^{Se} (45.8 mg, 0.14 mmol), NaOAc (12.6 mg, 0.15 mmol) and NH_4PF_6 (25.1 mg, 0.15 mmol) in acetonitrile (15 mL) was heated to reflux for 30 min. The orange suspension was cooled to room temperature and concentrated in vacuum. The resulting solid was filtered and washed with water and diethyl ether to give an orange solid. Yield: 0.098 g (93%)

^{1}H NMR (400 MHz, DMSO-d$_6$, 32 °C): δ = 1.28 (t, J = 7.1 Hz, 3H, NCH_2CH_3), 1.42 (t, J = 7.2 Hz, 3H, NCH_2CH_3), 3.94 (q, J = 7.1 Hz, 2H, NCH_2CH_3), 3.97 (q, J = 7.2 Hz, 2H, NCH_2CH_3), 7.98 (dd, J = 8.1, 5.3 Hz, 1H, H3- or H8-phen), 8.24 (d, J = 7.9 Hz, 1H, H3- or H8-phen), 8.30 (m, 4H, H-2, H-3), 8.62 (dd, J = 5.3, 0.9 Hz, 1H, H2- or H9-phen), 8.91 (dd, J = 8.1, 0.6 Hz, 1H, H4- or H7-phen), 8.97 (m, 2H, H4- or H7-phen) ppm. ^{31}P{^{1}H} NMR (243 MHz, DMSO-d$_6$, 25 °C): δ = −144.2 (sept, J = 711.2 Hz, PF_6) ppm. HR-ESI-MS: m/z (obs., calc.) = 613.9920, 613.9923 $[M]^+$. X-ray quality crystals were obtained by slow diffusion of diethyl ether into a saturated DMSO solution of the complex.

***cis*-[Pd{4-NO$_2$C$_6$H$_4$C(O)NC(S)NEt$_2$}(1,10-Phen)]PF$_6$.** This was prepared as above from [PdCl$_2$(1,10-Phen)] (50.0 mg,

0.14 mmol), HL^S (39.3 mg, 0.14 mmol), NaOAc (12.6 mg, 0.15 mmol) and NH_4PF_6 (25.1 mg, 0.15 mmol). The product was obtained as an orange solid in 79% yield (0.078 g). ^{1}H NMR (600 MHz, DMSO-d_6): δ = 1.28 (t, J = 7.1 Hz, 3H, NCH_2CH_3), 1.41 (t, J = 7.1 Hz, 3H, NCH_2CH_3),), 3.92 (q, J = 7.1 Hz, 2H, NCH_2CH_3), 3.97 (q, J = 7.1 Hz, 2H, NCH_2CH_3), 8.06 (dd, J = 8.1, 5.3 Hz, 1H, H3- or H8-phen), 8.22 (d, J = 8.8 Hz, 1H, H5- or H6-phen), 8.25 (dd, J = 8.2, 5.1 Hz, 1H, H8- or H3-phen), 8.27 (d, J = 8.8 Hz, 1H, H5- or H6-phen), 8.30 (d, J = 9.0 Hz, 2H, H-2), 8.33 (d, J = 9.0 Hz, 2H, H-3), 8.66 (dd, J = 5.3, 1.0 Hz, 1H, H2- or H9-phen), 8.73 (dd, J = 8.2, 0.9 Hz, 1H, H4- or H7-phen), 8.99 (dd, J = 8.2, 1.0 Hz, 1H, H4- or H7-phen), 9.02 (dd, J = 5.1, 1.1 Hz, 1H, H2- or H9-phen) ppm. ^{31}P{^{1}H} NMR (243 MHz, DMSO-d_6): δ = −144.2 (sept, J = 711.2 Hz, PF_6) ppm. HR-ESI-MS: m/z (obs., calc.) = 566.0474, 566.0478 $[M]^+$. X-ray quality crystals were obtained by slow diffusion of diethyl ether into a saturated acetonitrile solution of the complex.

Preparation of the ruthenium complexes

[Ru(*p*-cym){4-$NO_2C_6H_4C(O)NC(Se)NEt_2$}($PPh_3$)]$PF_6$. A mixture containing $[Ru(p\text{-cym})Cl_2]_2$ (50 mg, 0.082 mmol), HL^{Se} (53.6 mg, 0.163 mmol), Et_3N (23 μL, 0.165 mmol), Ph_3P (43 mg, 0.164 mmol) and NH_4PF_6 (29 mg, 0.179 mmol) in methanol (15 mL) was heated to reflux for 15 min. Addition of water to the red solution gave an orange precipitate. This was isolated by filtration and was washed with water and diethyl ether and subsequently dried in air. Yield: 0.132 g (84%). ^{1}H NMR (400 MHz, $CDCl_3$): δ = 1.11 (d, J = 6.9 Hz, 3H, $CH(CH_3)_2$), 1.20 (d, J = 6.9 Hz, 3H, $CH(CH_3)_2$), 1.28 (t, J = 7.1 Hz, 3H, NCH_2CH_3), 1.40 (t, J = 7.2 Hz, 3H, NCH_2CH_3), 1.91 (s, 3H, CCH_3), 2.54 (sept, J = 6.9 Hz, 1H, $CH(CH_3)_2$), 3.67 (dq, J = 13.2, 7.1 Hz, 1H, NCH_2CH_3), 3.92 (m, 2H, NCH_2), 4.35 (dq, J = 14.2, 7.1 Hz, 1H, NCH_2CH_3), 5.17 (d, J = 6.1 Hz, 1H, H-3 cym), 5.65 (m, 2H, H-2 cym, H-3′ cym), 5.72 (dd, J = 6.2, 1.0 Hz, 1H, H-2′ cym), 7.33–7.46 (m, 15H, PPh_3), 7.61 (d, J = 9.0 Hz, 2H, H-2), 8.03 (d, J = 8.9 Hz, 2H, H-3) ppm. ^{31}P{^{1}H} NMR (162 MHz, $CDCl_3$): 39.5 (PPh_3), −144.2 (sept, $^1J_{P-F}$ = 716.1 Hz, PF_6) ppm. ^{13}C{^{1}H} NMR (101 MHz, $CDCl_3$): δ = 13.0 (NCH_2CH_3), 13.4 (NCH_2CH_3), 18.0 (CCH_3), 22.0 ($CH(CH_3)_2$), 22.2 ($CH(CH_3)_2$), 31.2 (CH), 46.4 (NCH_2CH_3), 49.5 (NCH_2CH_3), 89.8 (d, $^2J_{P-C}$ = 3.2 Hz, C-3 cym), 90.0 (d, $^2J_{P-C}$ = 7.1 Hz, C-2 cym), 90.9 (C-3′ cym), 92.5 (d, $^2J_{P-C}$ = 1.5 Hz, C-2′ cym), 98.7 (C-4 cym), 114.8 (d, $^2J_{P-C}$ = 4.2 Hz, C-1 cym), 122.8 (C-3), 128.8 (d, $^3J_{P-C}$ = 10.1 Hz, *m*-PPh_3), 129.7 (C-2), 131.0 (d, $^1J_{P-C}$ = 47.8 Hz, i-PPh_3), 131.1 (d, $^4J_{P-C}$ = 2.4 Hz, *p*-PPh_3), 133.9 (d, $^2J_{P-C}$ = 9.8 Hz, *o*-PPh_3), 141.5 (C-1), 149.3 (C-4), 169.8 (d, $^3J_{P-C}$ = 4.2 Hz, C–Se), 170.7 (C–O) ppm. ^{77}Se NMR (76 MHz, DMSO-d_6): δ = −26 ppm. HR-ESI-MS: m/z (obs., calc.) = 826.1241, 826.1251 $[M]^+$, 564.0341, 564.0339 $[M - PPh_3]^+$. Crystals suitable for X-ray diffraction were grown by slow diffusion of diethyl ether into a CH_2Cl_2 and $CDCl_3$ mixture of the complex.

[Ru(*p*-cym){4-$NO_2C_6H_4C(O)NC(S)NEt_2$}(PPh_3)]PF_6. This was prepared as above using $[Ru(p\text{-cym})Cl_2]_2$ (50 mg, 0.082 mmol), HL^S (46.4 mg, 0.165 mmol), Ph_3P (43 mg, 0.164 mmol), Et_3N (23 μL, 0.165 mmol) and NH_4PF_6 (29 mg, 0.179 mmol). The product was obtained as a red solid in 38% yield (0.058 g). ^{1}H NMR (400 MHz, $CDCl_3$): δ = 1.17 (d, J = 6.9 Hz, 3H, $CH(CH_3)_2$), 1.20 (t, J = 6.9 Hz, 3H, NCH_2CH_3), 1.22 (d, J = 6.9 Hz, 3H, $CH(CH_3)_2$), 1.32 (t, J = 7.1 Hz, 3H, NCH_2CH_3), 1.83 (s, 3H, CCH_3 cym), 2.66 (sept, J = 6.9 Hz, 1H, $CH(CH_3)_2$), 3.67 (m, 2H, NCH_2CH_3), 3.86 (dq, J = 14.2, 7.1 Hz, 2H, NCH_2CH_3), 4.03 (dq, J = 14.2, 7.1 Hz, 1H, NCH_2), 5.26 (d, J = 6.1 Hz, 1H, H-3 cym, H-3′ cym), 5.42 (d, J = 6.1 Hz, 1H, H-3 cym, H-3′ cym), 5.70 (dd, J = 6.1, 0.9 Hz, 1H, H-2 cym, H-2′ cym), 5.82 (d, J = 6.2, 1.0 Hz, 1H, H-2 cym, H-2′ cym), 7.34–7.45 (m, 15H, PPh_3), 7.81 (d, J = 8.9 Hz, 2H, H-2, 8.11 (d, J = 8.9 Hz, 2H, H-3) ppm. ^{31}P{^{1}H} NMR (162 MHz, $CDCl_3$): 37.9 (PPh_3), −144.1 (sept, $^1J_{P-F}$ = 716.1 Hz, PF_6) ppm. ^{13}C{^{1}H} NMR (101 MHz, $CDCl_3$,): δ = 12.8 (NCH_2CH_3), 13.2 (NCH_2CH_3), 18.0 (CCH_3), 21.9 ($CH(CH_3)_2$), 22.2 ($CH(CH_3)_2$), 31.0 (CH), 46.0 (NCH_2CH_3), 47.2 (NCH_2CH_3), 87.8 (C-3 cym), 91.0 (d, $^2J_{P-C}$ = 5.8 Hz, C-2 cym), 92.7 (C-3′ cym), 93.9 (d, $^2J_{P-C}$ = 2.7 Hz, C-2′ cym), 102.2 (C-4 cym), 115.6 (d, $^2J_{P-C}$ = 6.4 Hz, C-1 cym), 123.0 (C-3), 128.8 (d, $^3J_{P-C}$ = 10.1 Hz, *m*-PPh_3), 129.7 (C-2), 130.3 (d, $^1J_{P-C}$ = 47.9 Hz, i-PPh_3), 131.2 (d, $^4J_{P-C}$ = 2.4 Hz, *p*-PPh_3), 134.0 (d, $^2J_{P-C}$ = 9.6 Hz, *o*-PPh_3), 142.0 (C-1), 149.4 (C-4), 169.2 (C–O), 173.2 (d, $^3J_{P-C}$ = 2.0 Hz, C–S) ppm. HR-ESI-MS: m/z (obs., calc.) = 778.1791, 778.1806 $[M]^+$, 516.0889, 516.0895 $[M - PPh_3]^+$. Crystals suitable for X-ray diffraction were grown by slow diffusion of diethyl ether into a $CDCl_3$ solution of the complex.

Biological activity

Compounds. All compounds were dissolved in dmso, aliquoted and stored at −20 °C. Prior to use solutions of the respective compound were diluted at least 1 : 1000 with cell culture medium. Dmso in the appropriate concentration did not induce any effect on the cell lines.

Cell lines. The leukemic cell lines were purchased from DSMZ – German Collection of Microorganisms and Cell Cultures, Braunschweig, Germany. The mammary carcinoma cell lines were kindly provided by the Institute of Pharmacy, Free University of Berlin. The ovarian carcinoma cell lines were kindly provided by the Department of Gynecology, Medical University Innsbruck. The acute myeloid leukemia cell line HL-60 as well as the chronic myeloid leukemia cell line K-562, the mammary carcinoma cell lines MCF-7 and MDA-MB231 as well as the ovarian carcinoma cell lines A2780 (cisplatin-sensitive and cisplatin-resistant) were grown in RPMI 1640 without phenol red (PAA Laboratories, Pasching, Austria), supplemented with glutamine (2 mM), penicillin (100 U mL^{-1}), streptomycin (100 μg mL^{-1}) and fetal bovine serum (FBS; 10%; all from Invitrogen Corporation, Gibco, Paisley, Scotland) at 37 °C in a 5% CO_2/95% air atmosphere and fed twice weekly. Cisplatin (1 μM) was added to the cisplatin-resistant A-2780 cell line every third passage. The acute lymphatic leukemia cell line SUP-B15 was grown in Mc Coy's 5A medium (Invitrogen) and supplemented with 20% FBS.

Analysis of metabolic activity and proliferation. Logarithmically growing cells were resuspended in culture medium at 1 × 10^6 cells per mL and plated in triplicate in U-bottomed or flat-bottomed microtiter plates (50 μL; Falcon, Becton Dickinson, Franklin Lakes, NJ, USA). Various concen-

trations of compounds were added one hour thereafter. After a three-day culture at 37 °C in a 5% CO_2/95% air atmosphere cultures were analyzed for metabolic activity using a modified 3-(4,5-dimethylthiazol-2-yl)-2,5-diphenyltetrazolium bromide (MTT) assay (EZ4U kit; Biomedica, Vienna, Austria) according to the manufacturer's instructions and for cellular proliferation using [methyl-^{3}H]-thymidine uptake. Metabolic activity and proliferation in the absence of the compound was set to 100%.

Analysis of apoptosis. The plates for apoptosis were prepared analogously as described above and were evaluated with an enzyme-linked immunoadsorbent assay (ELISA) using the ssDNA apoptosis kit (Chemicon International, Hofheim, Germany) according to the manufacturer's instructions. Apoptosis rate was evaluated by dividing the optical density of the wells measured in the plates for ssDNA apoptosis by the optical density of the wells for metabolic activity. Apoptosis in the absence of the compounds was set to 1.

Detection of morphological changes. 3×10^6 cells were adjusted to 1×10^6 cells per ml, placed in a 12-well plate and incubated at 37 °C in a humidified 5% CO_2/95% air atmosphere for 24 hours to let the cells adhere. After 24 hours 10 μM compound was added and the cells were cultivated for another 24 hours. Every 30 minutes a picture was made by JuLI™ Live cell imaging system (NanoEnTek, Seoul, Korea).

Measurement of intracellular ROS formation. SUP-B15 cells (1×10^6 cells per well) were incubated with 10 μM of the respective compound for two hours at 37 °C in a humidified 5% CO_2/95% air atmosphere, washed and treated for further 15 minutes with 5 μL of a 5 mM dihydroethidium solution (Sigma, St Louis, MO, USA) in 1 mL phosphate-buffered saline (PBS) + 1% bovine albumin (Ortho-Clinical Diagnostics, High Wycombe, UK). After another wash cells were resuspended in 500 μL PBS + 1% bovine albumin and analyzed immediately by flow cytometry (FACSCalibur, Becton Dickinson, San José, CA, USA).

Statistical analysis. The Wilcoxon Rank Sum Test was used to analyze the differences between proliferation, metabolic activity, apoptosis and ROS production in the absence and the presence of a variable concentration of the test compounds (NCSS software, Kaysville, UT, USA).

Conflicts of interest

There are no conflicts to declare.

Acknowledgements

FM gratefully acknowledges a visiting scientist award from the Spanish *CEI TRIANGULAR-E*^{3} *los horizontes del hombre* program. The authors wish to thank Petra Schumacher and Brigitte Floegel for excellent technical assistance.

References

1 I. B. Douglass, *J. Am. Chem. Soc.*, 1937, **59**, 740–742.
2 I. B. Douglass and F. B. Dains, *J. Am. Chem. Soc.*, 1934, **56**, 719–721.
3 J. Stach, R. Kirmse, A. Heinrich, W. Dietzsch, J. Hartung and L. Beyer, *Z. Chem.*, 1983, **23**, 453–454.
4 M. Schuster and K. H. König, *Fresenius' Z. Anal. Chem.*, 1988, **331**, 383–386.
5 J. Akhtar, J. C. Bruce, M. A. Malik, K. R. Koch, M. Afzaal and P. O'Brien, *Mater. Res. Soc. Symp. Proc.*, 2009, **1148E**, 1148.
6 F. Fuge, C. Lehmann and F. Mohr, *J. Organomet. Chem.*, 2009, **694**, 2395–2401.
7 M. Petrich, J. L. Cortina, J. Hartung, M. Aguilar, A. Sastre, L. Beyer and K. Gloe, *Solvent Extr. Ion Exch.*, 1993, **11**, 51–66.
8 M. Gielen and E. R. T. Tiekink, *Metallotherapeutic Drugs & Metal-based Diagnostic Agents*, John Wiley & Sons, Chichester, 2005.
9 S. J. Berners Price, C. K. Mirabelli, R. K. Johnson, M. R. Mattern, F. L. McCabe, L. F. Faucette, C. Sung, P. J. Sadler and S. T. Crooke, *Cancer Res.*, 1986, **46**, 5486–5493.
10 V. Gandin, A. P. Fernandes, M. P. Rigobello, B. Dani, F. Sorrentino, F. Tisato, M. Bjornstedt, A. Bindoli, A. Sturaro, R. Rella and C. Marzano, *Biochem. Pharmacol.*, 2010, **79**, 90–101.
11 E. R. T. Tiekink, *Crit. Rev. Oncol. Hemat.*, 2002, **42**, 225–248.
12 E. R. T. Tiekink, *Gold Bull.*, 2003, **36**, 117–124.
13 *Gold chemistry. Applications and future directions in the life sciences*, ed. F. Mohr, Wiley-VCH, Weinheim, 2009.
14 S. Medici, M. Peana, V. M. Nurchi, J. I. Lachowicz, G. Crisponi and M. A. Zoroddu, *Coord. Chem. Rev.*, 2015, **284**, 329–350.
15 S. Miranda, E. Vergara, F. Mohr, D. de Vos, E. Cerrada, A. Mendía and M. Laguna, *Inorg. Chem.*, 2008, **47**, 5641–5648.
16 E. Schuh, C. Pflüger, A. Citta, A. Folda, M. P. Rigobello, A. Bindoli, A. Casini and F. Mohr, *J. Med. Chem.*, 2012, **55**, 5518–5528.
17 G. Binzet, H. Arslan, U. Flörke, N. Külcü and N. Duran, *J. Coord. Chem.*, 2006, **59**, 1395–1406.
18 Y. Nural, R. Kilincarslan, H. A. Dondas, B. Cetinkaya, M. S. Serin, R. Grigg, T. Ince and C. Kilner, *Polyhedron*, 2009, **28**, 2847–2854.
19 A. C. Tenchiu, M. Iliş, F. Dumitraşcu, A. C. Whitwood and V. Cîrcu, *Polyhedron*, 2008, **27**, 3537–3544.
20 V. Circu, D. Manaila-Maximean, C. Rosu, M. Ilis, Y. Molard and F. Dumitrascu, *Liq. Cryst.*, 2009, **36**, 123–132.
21 M. Cusumano, M. L. Di Pietro and A. Giannetto, *Inorg. Chem.*, 2006, **45**, 230–235.
22 M. Cusumano, M. L. Di Pietro, A. Giannetto and P. A. Vainiglia, *J. Inorg. Biochem.*, 2005, **99**, 560–565.
23 M. Cusumano, M. L. Di Pietro, A. Giannetto and P. A. Vainiglia, *Eur. J. Inorg. Chem.*, 2005, 278–284.

24 M. N. Alam and F. Huq, *Coord. Chem. Rev.*, 2016, **316**, 36–67.
25 C. S. Allardyce, P. J. Dyson, D. J. Ellis and S. L. Heath, *Chem. Commun.*, 2001, 1396–1397.
26 C. Scolaro, A. Bergamo, L. Brescacin, R. Delfino, M. Cocchietto, G. Laurenczy, T. J. Geldbach, G. Sava and P. J. Dyson, *J. Med. Chem.*, 2005, **48**, 4161–4171.
27 C. A. Vock, W. H. Ang, C. Scolaro, A. D. Phillips, L. Lagopoulos, L. Juillerat-Jeanneret, G. Sava, R. Scopelliti and P. J. Dyson, *J. Med. Chem.*, 2007, **50**, 2166–2175.
28 A. Dorcier, W. H. Ang, S. Bolaño, L. Gonsalvi, L. Juillerat-Jeannerat, G. Laurenczy, M. Peruzzini, A. D. Phillips, F. Zanobini and P. J. Dyson, *Organometallics*, 2006, **25**, 4090–4096.
29 A. K. Renfrew, A. D. Phillips, A. E. Egger, C. G. Hartinger, S. S. Bosquain, A. A. Nazarov, B. K. Keppler, L. Gonsalvi, M. Peruzzini and P. J. Dyson, *Organometallics*, 2009, **28**, 1165–1172.
30 R. S. Correa, K. M. de Oliveira, F. G. Delolo, A. Alvarez, R. Mocelo, A. M. Plutin, M. R. Cominetti, E. E. Castellano and A. A. Batista, *J. Inorg. Biochem.*, 2015, **150**, 63–71.
31 B. Tang, D. Wan, S. H. Lai, H. H. Yang, C. Zhang, X. Z. Wang, C. C. Zeng and Y. J. Liu, *J. Inorg. Biochem.*, 2017, **173**, 93–104.
32 L. Chen, G. Li, F. Peng, X. Jie, G. Dongye, K. Cai, R. Feng, B. Li, Q. Zeng, K. Lun, J. Chen and B. Xu, *Oncotarget*, 2016, **7**, 80716–80734.
33 G. Roebisch, E. Ludwig and W. Bansse, *Z. Anorg. Allg. Chem.*, 1982, **493**, 26–32.
34 J. Sieler, R. Richter, E. Hoyer, L. Beyer, O. Lindqvist and L. Andersen, *Z. Anorg. Allg. Chem.*, 1990, **580**, 167–174.
35 K. H. König, M. Schuster, G. Schneeweis and B. Steinbrech, *Fresenius' Z. Anal. Chem.*, 1984, **319**, 66–69.
36 S. Pisiewicz, J. Rust, C. W. Lehmann and F. Mohr, *Polyhedron*, 2010, **29**, 1968–1972.
37 M. Schuster and K. H. Koenig, *Fresenius' Z. Anal. Chem.*, 1988, **331**, 383–386.
38 N. Gunasekaran and R. Karvembu, *Inorg. Chem. Commun.*, 2010, **13**, 952–955.
39 E. Guerrero, S. Miranda, S. Luttenberg, N. Frohlich, J. M. Koenen, F. Mohr, E. Cerrada, M. Laguna and A. Mendia, *Inorg. Chem.*, 2013, **52**, 6635–6647.
40 D. Dolfen, K. Schottler, V. Seied-Mojtaba, M. A. Jakupec, B. K. Keppler, E. R. T. Tiekink and F. Mohr, *J. Inorg. Biochem.*, 2008, **102**, 2067–2071.
41 P. Bippus, M. Skocic, M. A. Jakupec, B. K. Keppler and F. Mohr, *J. Inorg. Biochem.*, 2011, **105**, 462–466.
42 A. Molter, J. Rust, C. W. Lehmann, G. Deepa, P. Chiba and F. Mohr, *Dalton Trans.*, 2011, **40**, 9810–9820.
43 E. Schuh, S. M. Valiahdi, M. A. Jakupec, B. K. Keppler, P. Chiba and F. Mohr, *Dalton Trans.*, 2009, 10841–10845.
44 R. Rubbiani, E. Schuh, A. Meyer, J. Lemke, J. Wimberg, N. Metzler-Nolte, F. Meyer, F. Mohr and I. Ott, *MedChemComm*, 2013, **4**, 942–948.
45 T. B. Wei, H. Wang, Q. Lin and Y. M. Zhang, *Chin. J. Org. Chem.*, 2005, **25**, 1565–1569.
46 J. C. Bruce, N. Revaprasadu and K. R. Koch, *New J. Chem.*, 2007, **31**, 1647–1653.
47 S. Saeed, N. Rashid, J. P. Jasinski, R. J. Butcher and H. Rizwan, *Acta Crystallogr., Sect. E: Struct. Rep. Online*, 2010, **66**, O2589–U2710.
48 M. R. J. Elsegood, M. B. Smith and N. M. Sanchez-Ballester, *Acta Crystallogr., Sect. E: Struct. Rep. Online*, 2006, **62**, M2838–M2840.
49 P. L. Andreu, J. A. Cabeza, D. Miguel, V. Riera, M. A. Villa and S. Garciagranda, *J. Chem. Soc., Dalton Trans.*, 1991, 533–536.
50 J. F. Arambula, R. McCall, K. J. Sidoran, D. Magda, N. A. Mitchell, C. W. Bielawski, V. M. Lynch, J. L. Sessler and K. Arumugam, *Chem. Sci.*, 2016, **7**, 1245–1256.
51 C. Sánchez-de-Diego, I. Mármol, R. Pérez, S. Gascón, M. J. Rodriguez-Yoldi and E. Cerrada, *J. Inorg. Biochem.*, 2017, **166**, 108–121.
52 M. Altaf, M. Monim-Ul-Mehboob, A. N. Kawde, G. Corona, R. Larcher, M. Ogasawara, N. Casagrande, M. Celegato, C. Borghese, Z. H. Siddik, D. Aldinucci and A. A. Isab, *Oncotarget*, 2017, **8**, 490–505.
53 J. Yellol, S. A. Pérez, A. Buceta, G. Yellol, A. Donaire, P. Szumlas, P. J. Bednarski, G. Makhloufi, C. Janiak, A. Espinosa and J. Ruiz, *J. Med. Chem.*, 2015, **58**, 7310–7327.
54 L. S. Flocke, R. Trondl, M. A. Jakupec and B. K. Keppler, *Invest. New Drugs*, 2016, **34**, 261–268.
55 C. C. Zeng, S. H. Lai, J. H. Yao, C. Zhang, H. Yin, W. Li, B. J. Han and Y. J. Liu, *Eur. J. Med. Chem.*, 2016, **122**, 118–126.
56 P. Banerjee, P. Majumder, S. Halder, M. G. Drew, S. Bhattacharya and S. Mazumder, *Free Radical Res.*, 2015, **49**, 253–268.
57 R. Usón, A. Laguna and M. Laguna, *Inorg. Synth.*, 1989, **26**, 85–91.
58 F. R. Hartley, *Organomet. Chem. Rev., Sect. A*, 1970, **6**, 119–137.
59 M. A. Bennett, T. N. Huang, T. W. Matheson and A. K. Smith, *Inorg. Synth.*, 1982, **21**, 74–78.
60 W. Hernandez, E. Spodine, A. Vega, R. Richter, J. Griebel, R. Kirmse, U. Schroder and L. Beyer, *Z. Anorg. Allg. Chem.*, 2004, **630**, 1381–1386.
61 *CrysalisPro*, Rigaku Oxford Diffraction, Oxford, UK, 2016.
62 O. V. Dolomanov, L. J. Bourhis, R. J. Gildea, J. A. K. Howard and H. Puschmann, *J. Appl. Crystallogr.*, 2009, **42**, 339–341.